The standard deviation of an observation unit weight defined as $[\sum(|F_o| - |F_c|)^2/(m - n)]^{1/2}$ was 3.70, where the number of reflections (m) was 3980 and the number of refinement parameters (n) was 467. The positional parameters obtained from the last cycle of refinement were listed in Table VI with the associated standard deviations estimated from the inverse matrix. Anisotropic thermal parameters for non-hydrogen atoms and a listing of the observed and calculated structure amplitudes are available as supplementary material.[24]

(24) See paragraph at the end of this paper regarding supplementary material.

Acknowledgment. We thank Dr. T. Tanase for helpful discussion on X-ray crystallographic study.

Registry No. 1, 24013-40-9; 2, 105536-94-5; 3, 105560-54-1; 4, 114378-02-8; 5, 114378-03-9; 6, 114378-04-0; 7, 114394-74-0; 8, 105536-96-7; 9, 101299-76-7; 10, 105059-23-2; Ru, 7440-18-8; Co, 7440-48-4.

Supplementary Material Available: A listing of anisotropic displacement parameters for non-hydrogen atoms (1 page); a listing of observed and calculated structure factors (10 pages). Ordering information is given on any current masthead page.

Synthesis, Structures, and Solution Dynamics of Mononuclear and Dinuclear (η^5-Indenyl)rhodium Complexes of Octafluorocyclooctatetraene. Crystal and Molecular Structures of $[Rh(\eta^5\text{-}C_9H_7)(1,2,5,6\text{-}\eta\text{-}C_8F_8)]$, $\{[Rh(\eta^5\text{-}C_9H_7)]_2[\mu\text{-}(1,5,6\text{-}\eta\text{:}2\text{–}4\text{-}\eta\text{-}C_8F_8)](Rh\text{–}Rh)\}$, $\{[Rh(\eta^5\text{-}C_9H_7)]_2[\mu\text{-}(1,5,6\text{-}\eta\text{:}2\text{–}4\text{-}\eta\text{-}C_8F_7H)](Rh\text{–}Rh)\}$, and $\{[Rh(\eta^5\text{-}C_9H_7)(CO)][Rh(\eta^5\text{-}C_9H_7)][\mu\text{-}(1,2,5,6\text{-}\eta\text{:}7,8\text{-}\eta\text{-}C_8F_8]\}$

Richard T. Carl,[1a,2] Russell P. Hughes,*[1a] Arnold L. Rheingold,[1b] Todd B. Marder,[1c] and Nicholas J. Taylor[1c]

Departments of Chemistry, Dartmouth College, Hanover, New Hampshire 03755, University of Delaware, Newark, Delaware 19716, and The Guelph-Waterloo Centre for Graduate Work in Chemistry, Waterloo Campus, Department of Chemistry, University of Waterloo, Waterloo, Ontario N2L 3G1, Canada

Received November 16, 1987

The molecular structure of (indenyl)(1,2,5,6-η-octafluorocyclooctatetraene)rhodium (**5**) has been determined. The crystal is triclinic, $P\bar{1}$, with a = 8.445 (1) Å, b = 8.850 (1) Å, c = 10.142 (1) Å, α = 85.22 (1)°, β = 81.63 (1)°, γ = 89.35 (1)°, V = 747.3 (2) Å^3, and Z = 2. Analysis of the solid-state structure in terms of the degree of slip folding of the indenyl ligand indicates that the indenyl ligand is partially slipped toward η^3-coordination and that octafluorocyclooctatetraene (OFCOT) is a slightly better acceptor ligand than ethylene. The slippage of the indenyl ligand in solution has also been analyzed from the $^{13}C\{^1H\}$NMR spectral data for **5**. Line-shape analysis of the variable-temperature ^{19}F NMR spectrum of **5** allows a value of E_a for indenyl rotation of 8.6 ± 0.8 kcal/mol to be calculated. Similar variable-temperature ^1H NMR studies of the hydrocarbon analogue $Rh(C_9H_7)(1,2,5,6\text{-}C_8H_8)$ (**10**) produce an E_a for indenyl rotation of 9.4 ± 0.7 kcal/mol. Reaction of **5** with $Rh(C_9H_7)(C_2H_4)_2$ (**9**) produces the red dinuclear complex **12** whose solid-state molecular structure has also been determined by single-crystal X-ray diffraction: monoclinic, $P2_1/c$, a = 8.170 (1) Å, b = 13.770 (1) Å, c = 20.079 (3) Å, β = 96.22 (1)°, V = 2245.6 (5) Å^3, Z = 4. Solution studies of **12** using variable-temperature ^{19}F NMR indicate that the bridging OFCOT ligand is fluxional via a process (E_a = 16.3 ± 0.4 kcal/mol) which interchanges the two enantiomorphs of **12**, by pairwise exchange of fluorine environments without concomitant interchange of the two rhodium environments. A mechanism consistent with these observations is proposed. The rhodium–rhodium bond in **12** is cleaved by CO to produce a mixture of **18** (major isomer) and **19** (minor isomer) and by C_2H_4 to produce the analogous complex **20**. Complexes **18–20** revert to **12** thermally and are probably good models for the intermediate en route to formation of **12** from **5** and **9**. The molecular structure of **18** has been confirmed by a single-crystal X-ray diffraction experiment: triclinic, $P\bar{1}$, a = 8.947 (1) Å, b = 9.840 (3) Å, c = 14.081 (3) Å, α = 96.94 (2)°, β = 102.11 (2)°, γ = 97.63 (2)°, V = 1187.2 (4) Å^3, Z = 2. Complex **12** also undergoes a kinetically selective fluorine for hydrogen exchange reaction during chromatography on various supports. The structure of the principal product **21** has also been determined crystallographically: monoclinic, $P2_1/c$, a = 11.375 (3) Å, b = 14.277 (3) Å, c = 14.211 (3) Å, β = 104.55°, V = 2233.8 (9) Å^3, Z = 4.

Introduction

The coordination chemistry of cyclooctatetraene (COT) and many of its hydrocarbon relatives has been thoroughly studied and has resulted in the synthesis of molecules that have provided an increased understanding of bonding and dynamic behavior of coordinated hydrocarbons.[3] We have been studying the transition-metal chemistry of the fluorocarbon analogue octafluorocyclooctatetraene (OFCOT)

(1) (a) Dartmouth College. (b) University of Delaware. (c) University of Waterloo.

(2) Present address: Nicolet Analytical Instruments, 5225 Verona Road, P.O. Box 4508, Madison, WI 53711-0508.

(3) For reviews of the organic and organometallic chemistry of cyclooctatetraene see: Fray, G. I.; Saxton, R. G. *The Chemistry of Cyclooctatetraene and Its Derivatives*; Cambridge University Press: Cambridge, 1978. Deganello, G. *Transition Metal Complexes of Cyclic Polyolefins*; Academic: New York, 1979.

0276-7333/88/2307-1613$01.50/0

(1) whose synthesis[4] and molecular structure[5] have already been reported. In many cases the structures and chemistry of OFCOT complexes have proven to be significantly different from those of COT analogues, where such analogues in fact exist.

In a previous paper the syntheses of 1,2,5,6-η-OFCOT complexes containing the M(C_5H_5) fragment (M = Co, Rh) were described.[6] In each case the ground-state structure was found to be **2**, and no other ligation or valence isomers could be detected under conditions of thermal or photochemical activation. Isomers **3** and **4**, containing the bicyclo[4.2.0]octatriene valence isomer of OFCOT, could be generated by an alternative route but showed no proclivity for thermal or photochemical isomerization to complexes containing monocyclic OFCOT.[6] The η^5-indenyl analogue **5** was similarly prepared,[6] and more recently we described the synthesis of pentamethylcyclopentadienylcobalt and rhodium analogues **6**, their electrochemistry, and their photochemistry to afford isomers **7** resulting from a formal oxidative addition to the metal center.[7]

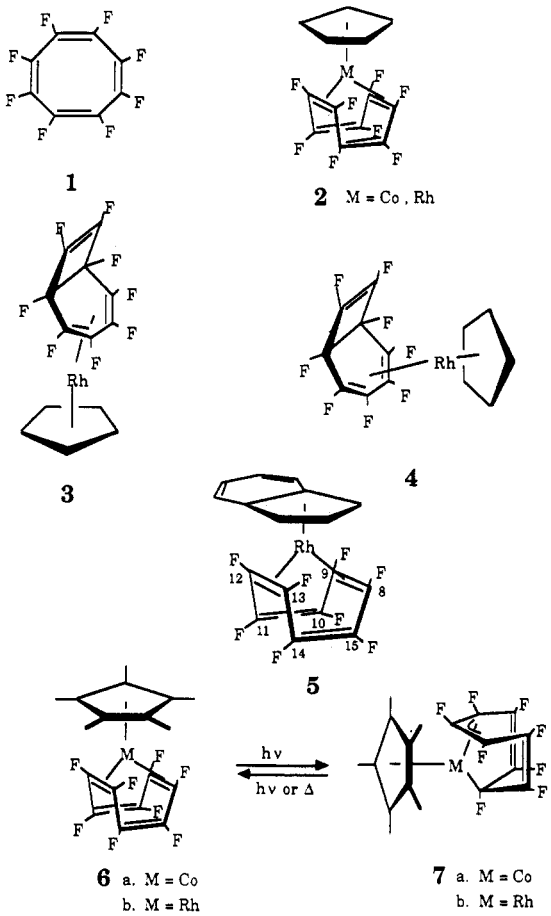

Recently, there has been interest in the enhanced reactivity of indenyl metal complexes as compared to their corresponding cyclopentadienyl analogues.[8-13] For example, Mo(η^5-C_9H_7)X(CO)$_3$ (X = halogen) has a higher reactivity toward ligand substitution than its cyclopentadienyl analogue.[10] It has been proposed that this enhanced reactivity is due to a slippage of the indenyl ligand from an η^5 to an η^3 bonding mode, thus making the metal center coordinatively unsaturated.[10-12] This proposal has received support from kinetic studies[11] as well as X-ray diffraction data.[12,13a] Presumably, some of the resonance energy that is lost in η^5 to η^3 slippage is recovered from the resonance energy of the benzene ring.[10] X-ray crystallographic data indicate that as the indenyl ring distorts from η^5 to η^3, the arene ring gradually folds out of the plane of the allylic fragment.[12,13a] Therefore, the slip folding of the C_5 ring can be used to quantify the degree of η^3-character of a particular system.[12c,13a]

Table I. Slip-Fold Parameters for Some Rh(η-C_9H_7)L_2 Complexes

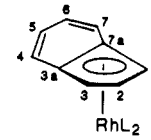

complex	Δ (Å)[e]	HA (deg)[a,e]	FA (deg)[a,e]
Rh(η-C_9H_7)(C_2H_4)$_2$[c]	0.160 (5)[a]	8.3 (4)	7.3 (4)
Rh(η-C_9H_7)(C_2H_4)$_2$[c]	0.161 (5)[a]	7.8 (4)	7.5 (4)
Rh(η-C_9H_7)(duroquinone)[d]	0.05 (2)	2 (1)	3 (1)
Rh(η-C_9H_7)(μ-PPh_2)$_2$$ZrCp_2$	0.227 (3)[a,b]	10.6 (3)	8.5 (3)

[a] As reported in ref 13. [b] As calculated from published crystallographic data.[12c] [c] Values for two independent molecules. [d] As calculated from published crystallographic data (Aleksandrov, G. G.; Struchkov, Yu. T. *Zh. Struct. Khim.* **1971**, *12*, 120). [e] Δ (Å) = [(d(Rh–C_{3a}) + d(Rh–C_{7a}))/2 – (d(Rh–C_3) + d(Rh–C_1))/2]. HA (hinge angle) = angle between normals to the least-squares planes defined by C_1, C_2, C_3 and C_1, C_{7a}, C_{3a}. FA (fold angle) = angle between normals to the least-squares plane defined by C_1, C_2, C_3, and C_{3a}, C_4, C_5, C_6, C_7, C_{7a}.

Marder et al. have developed a measure of the amount of slip folding based on X-ray crystallographic data of substituted indenyl complexes and have related this "slip-fold" distortion to the σ-donor/π-acceptor characteristics of the ligands.[13a] A good σ-donor ligand such as PMe_3 should stabilize η^3-coordination by its ability to donate electron density to the metal. Conversely, a good π-acceptor ligand would remove electron density from the metal center and favor η^5-coordination of the indenyl ligand.[13a] Table I defines the slip-fold parameters and presents the slip-folding data for a number of complexes.[13a] The larger the value of Δ, HA, and FA, the more distortion to an η^3-indenyl ligand and the better the σ-donating ability of the other ligands.

More conveniently and more relevant to solution chemistry, the slip-fold distortion of the indenyl ligand in solution can be calculated from the ^{13}C NMR spectral data.

(4) Lemal, D. M.; Buzby, J. M.; Barefoot, A. C., III; Grayston, M. W.; Laganis, E. D. *J. Org. Chem.* **1980**, *45*, 3118–3120.
(5) Laird, B. B.; Davis, R. E. *Acta Crystallogr., Sect. B: Struct. Crystallogr. Cryst. Chem.* **1982**, *B38*, 678–680.
(6) Doherty, N. M.; Ewels, B. E.; Hughes, R. P.; Samkoff, D. E.; Saunders, W. D.; Davis, R. E.; Laird, B. B. *Organometallics* **1985**, *4*, 1606–1611.
(7) Carl, R. T.; Doig, S. J.; Geiger, W. E.; Hemond, R. C.; Hughes, R. P.; Kelly, R. S.; Samkoff, D. E. *Organometallics* **1987**, *6*, 611–616.
(8) (a) Caddy, P.; Green, M.; O'Brien, E.; Smart, L. E.; Woodward, P. *J. Chem. Soc., Dalton Trans.* **1980**, 962–972. (b) Caddy, P.; Green, M.; O'Brien, E.; Smart, L. E.; Woodward, P. *Angew. Chem., Int. Ed. Engl.* **1977**, *16*, 648–649.
(9) Werner, H.; Feser, R. *Z. Naturforsch., B: Anorg. Chem., Org. Chem.* **1980**, *35B*, 689.
(10) (a) Hart-Davis, A. J.; White, C.; Mawby, R. J. *Inorg. Chim. Acta* **1970**, *4*, 1441. (b) Hart-Davis, A. J.; White, C.; Mawby, R. J. *J. Chem. Soc. A* **1969**, 2403–2407. (c) Jones, D. J.; Mawby, R. J. *Inorg. Chim. Acta* **1972**, *6*, 157.
(11) (a) Rerek, M. E.; Ji, L.-N.; Basolo, F. *J. Chem. Soc., Chem. Commun.* **1983**, 1208–1209. (b) Ji, L.-N.; Rerek, M. E.; Basolo, F. *Organometallics* **1984**, *3*, 740–745.
(12) (a) Faller, J. W.; Crabtree, R. H.; Habib, A. *Organometallics* **1985**, *4*, 929–935. (b) Merola, J. S.; Kacmarcik, R. T.; Van-Engan, D. *J. Am. Chem. Soc.* **1986**, *108*, 329–331. (c) Baker, R. T.; Tulip, T. H. *Organometallics* **1986**, *5*, 839–845.
(13) (a) Marder, T. B.; Calabrese, J. C.; Roe, D. C.; Tulip, T. H. *Organometallics* **1987**, *6*, 2012–2014. (b) Barr, R. D.; Green, M.; Marder, T. B.; Stone, F. G. A. *J. Chem. Soc., Dalton Trans.* **1984**, 1261.

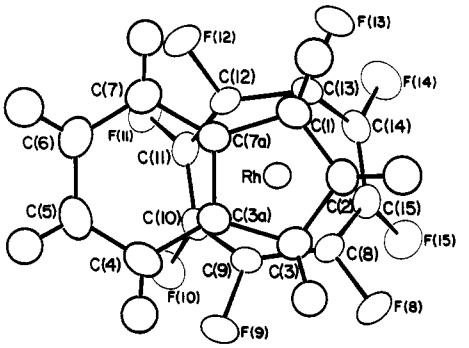

Figure 1. Molecular structure and atom labeling scheme for complex **5**.

Kohler[14] has noted that the hapticity of the indenyl ligand can be evaluated spectroscopically by comparing the ^{13}C NMR chemical shifts of the five-membered ring carbons in the metal complex with those of indene itself. It would appear that for η^3-indenyl ligands C(1–3) [see Table I for numbering] would be shielded while C(3a,7a) would not experience this shielding.[12c] Baker and Tulip have calculated the chemical shift difference $\Delta\delta(C) = \delta[C(\eta\text{-indenyl})] - \delta[C(\eta\text{-indenyl})\text{sodium}]$ for a number of d^6 and d^8 metal complexes, and the values correlate well with the structurally observed hapticity.[12c] A $\Delta\delta$(C3a,7a) of −20 to −40 ppm indicates a planar η^5-indenyl, of −10 to −20 ppm indicates a partially slipped η^5-indenyl, and of +5 to +30 ppm indicates η^3-indenyl ligands.[12c]

Perfluorinated ligands are thought to be good π-acceptors due to the electron-withdrawing effect of the fluorines.[15] As mentioned above, the σ-donating/π-accepting ability of a ligand can be determined by the slip-fold parameters of an indenyl complex containing this ligand. An ideal candidate for the study of the σ-donating/π-accepting ability of OFCOT would be [Rh(η-C_9H_7)(1,2,5,6-η-C_8F_8)] (**5**).[6] We have shown that apparent slippage of the indenyl ligand in **5** can facilitate entry of exogenous ligands such as *t*-BuNC, leading ultimately to the transannular ring-closure product **8**.[16]

Here we report the synthesis, structures, and solution dynamics of **5** and some dinuclear complexes derived from its reactions with the (indenyl)Rh fragment.

Results and Discussion

Structure and Solution Dynamics of the Mononuclear OFCOT Complex 5. Crystallization of **5** from hexane at −20 °C produced single crystals that were subjected to an X-ray diffraction study in order to determine the degree of slip folding. The solid-state structure and numbering scheme for **5** are shown in Figure 1. Fractional atomic coordinates are listed in Table II, and selected bond angles and lengths appears in Table III.

The metal center is bound to the C_8F_8 ring in a 1,2,5,6-η fashion as was previously suggested from NMR studies in solution.[6] There is substantial lengthening of the C=C bond upon coordination [C=C, coordinated (average) = 1.451 (8) Å vs C=C, uncoordinated (average) = 1.342 (8) Å]. This would indicate that OFCOT is a fairly good π-acceptor since coordination of the double bond to the metal center would populate the π^*-orbitals of the olefin, weakening the C=C bond. Additionally, the C–F distances for the fluorines attached to the coordinated carbons are also significantly longer than the C–F distances for the fluorines attached to the uncoordinated carbons [C–F, coordinated (average) = 1.360 (3) Å; C–F, uncoordinated (average) = 1.345 (3) Å]. This indicates partial rehybridization of the coordinated carbons toward sp^3.

For sp^2-hybridized carbon (planar geometry), the sum of the internal C–C–C angle and the two C–C–F angles

Table II
Fractional Atomic Coordinates (×10⁴) for Complex **5**

atom	x	y	z
Rh	2444.9 (2)	1832.4 (2)	2664.0 (2)
F(8)	5610 (2)	379 (2)	2778 (2)
F(9)	5310 (2)	2210 (2)	596 (2)
F(10)	5920 (2)	5137 (2)	1271 (2)
F(11)	3312 (2)	6481 (2)	2643 (2)
F(12)	567 (2)	4642 (2)	3117 (2)
F(13)	892 (2)	2817 (2)	5281 (2)
F(14)	3811 (3)	3692 (3)	6002 (2)
F(15)	6444 (2)	2341 (3)	4601 (2)
C(1)	124 (3)	618 (3)	2982 (3)
C(2)	1346 (4)	−468 (3)	2900 (3)
C(3)	2284 (4)	−215 (3)	1631 (3)
C(3A)	1486 (3)	903 (3)	830 (3)
C(4)	1831 (4)	1526 (3)	−505 (3)
C(5)	823 (4)	2598 (4)	−951 (3)
C(6)	−500 (4)	3115 (4)	−117 (3)
C(7)	−844 (3)	2568 (3)	1186 (3)
C(7A)	144 (3)	1431 (3)	1679 (3)
C(8)	4823 (3)	1717 (3)	2972 (3)
C(9)	4676 (3)	2709 (3)	1798 (2)
C(10)	4615 (3)	4350 (3)	1820 (2)
C(11)	3364 (3)	4989 (3)	2483 (3)
C(12)	2048 (3)	4059 (3)	3203 (3)
C(13)	2216 (3)	3067 (3)	4352 (2)
C(14)	3724 (4)	2958 (3)	4905 (3)
C(15)	4961 (3)	2313 (3)	4244 (3)

Hydrogen Atom Coordinates (Fractional, ×10³) and Isotropic Thermal Parameters (U_{iso}) for Complex **5**

atom	x	y	z	U_{iso}, Å²
H(1)	−67 (4)	71 (4)	375 (3)	68 (10)
H(2)	162 (4)	−117 (4)	360 (3)	64 (10)
H(3)	320 (4)	−81 (3)	130 (3)	58 (9)
H(4)	272 (4)	122 (4)	−106 (3)	55 (9)
H(5)	99 (4)	300 (3)	−185 (3)	64 (9)
H(6)	−126 (4)	386 (4)	−45 (3)	72 (10)
H(7)	−173 (4)	292 (3)	174 (3)	60 (9)

Table III. Selected Bond Distances (Å) and Angles (deg) for Complex 5[a]

(a) Bond Distances (Å)

Rh–C(1)	2.215 (3)	Rh–C(2)	2.227 (3)
Rh–C(3)	2.183 (3)	Rh–C(3A)	2.345 (3)
Rh–C(7A)	2.354 (2)	Rh–C(8)	2.077 (2)
Rh–C(9)	2.088 (2)	Rh–CENT	2.028 (3)
Rh–C(12)	2.099 (2)	Rh–C(13)	2.091 (2)
C(8)–C(9)	1.439 (4)	C(9)–C(10)	1.455 (4)
C(10)–C(11)	1.317 (4)	C(12)–C(13)	1.464 (4)
C(13)–C(14)	1.423 (4)	C(14)–C(15)	1.309 (4)
C(8)–F(8)	1.366 (3)	C(9)–F(9)	1.365 (3)
C(10)–F(10)	1.342 (3)	C(11)–F(11)	1.343 (3)
C(12)–F(12)	1.360 (3)	C(13)–F(13)	1.360 (3)
C(14)–F(14)	1.345 (3)	C(15)–F(15)	1.355 (3)

(b) Bond Angles (deg)

C(1)–C(2)–C(3)	107.74 (16)	C(7A)–C(1)–C(2)	108.77 (15)
C(3)–C(3A)–C(7A)	106.93 (15)	C(4)–C(3A)–C(7A)	119.87 (16)
C(1)–C(7A)–C(3A)	107.24 (15)	C(7)–C(7A)–C(3A)	120.02 (16)

[a] CENT = centroid of C(1), C(2), C(3), C(3a), C(7a).

(14) Kohler, F. H. *Chem. Ber.* **1974**, *107*, 570–574.
(15) (a) Cramer, R.; Kline, J. B.; Roberts, J. D. *J. Am. Chem. Soc.* **1969**, *91*, 2519–2524. (b) Guggenberger, L. J.; Cramer, R. *J. Am. Chem. Soc.* **1972**, *94*, 3779–3787. (c) Churchill, M. R.; Mason, R. *Proc. Chem. Soc.* **1964**, 226. (d) Churchill, M. R.; Mason, R. *Proc. R. Soc. London, Ser.* **1967**, *301*, 433. (e) Hoehn, H. H.; Pratt, L.; Watterson, K. F.; Wilkinson, G. *J. Chem. Soc.* **1961**, 2738–2745.
(16) Carl, R. T.; Hughes, R. P.; Samkoff, D. E. *Organometallics*, following paper in this issue.

Table IV. Comparison of the Bond Angle Sums (deg) at Coordinated and Uncoordinated Olefinic Carbon Atoms for Complex 5

coordinated		uncoordinated	
C(14)–C(13)–C(12)	121.31 (15)	C(14)–C(14)–C(15)	119.35 (16)
C(14)–C(13)–F(13)	114.03 (13)	C(13)–C(14)–F(14)	117.13 (13)
C(12)–C(13)–F(13)	117.19 (12)	C(15)–C(14)–F(14)	123.06 (15)
	352.53		359.54
C(11)–C(12)–C(13)	122.65 (12)	C(14)–C(15)–C(8)	119.79 (16)
C(13)–C(12)–F(12)	116.91 (12)	C(14)–C(15)–F(15)	122.66 (15)
C(11)–C(12)–F(12)	114.56 (15)	C(8)–C(15)–F(15)	117.00 (13)
	354.06		359.45
C(15)–C(8)–F(8)	114.19 (13)	C(9)–C(10)–F(10)	117.50 (12)
C(15)–C(8)–C(9)	121.35 (15)	C(11)–C(10)–F(10)	122.48 (14)
C(9)–C(8)–F(8)	116.83 (12)	C(9)–C(10)–C(11)	119.65 (15)
	352.37		359.63
C(8)–C(9)–C(10)	122.27 (14)	C(10)–C(11)–C(12)	120.30 (13)
C(8)–C(9)–F(9)	116.87 (12)	C(12)–C(11)–F(11)	117.25 (12)
C(10)–C(9)–F(9)	114.55 (12)	C(10)–C(11)–C(12)	120.30 (15)
	353.69		359.63

should equal 360°. For sp^3-hybridized carbon (tetrahedral geometry), the sum of the same three angles should equal 328.5°. A calculation of the sum of the relevant bond angles for **5** is shown in Table IV. The geometry around the uncoordinated carbons is planar, and the carbons can clearly be thought of as sp^2. However, the geometry around the coordinated carbons is not planar; the sum of the angles is less than 360°. Therefore, this criterion is also indicative of some rehybridization upon coordination.

It was expected that any rehybridization should also be reflected in the $^1J_{C-F}$ values observed in the $^{13}C\{^1H\}$ NMR spectrum. Curiously, the coupling constants of the coordinated carbons to the attached fluorines ($^1J_{C-F}$ = 289.9 Hz) are nearly identical with those of the uncoordinated carbons to their respective fluorines ($^1J_{C-F}$ = 290.9 Hz). By way of comparison, for the (pentamethylcyclopentadienyl)cobalt complex **6a** the coupling constant of the coordinated carbons to the attached fluorines is 281 Hz while $^1J_{C-F}$ for the uncoordinated carbons is 302 Hz.

Calculation of the slip parameter from the X-ray crystallographic data of **5** gives Δ = 0.150 Å, indicating that OFCOT is a moderately good σ-donor and a moderate π-acceptor by comparison with the slip parameters for the complexes in Table I. It is apparently a slightly better π-acceptor than ethylene as would be expected due to the electron-withdrawing nature of the fluorines.

Calculation of the slip parameter from the ^{13}C NMR spectral data of **5**, using the method of Baker and Tulip,[12c] gives a $\Delta\delta$(C3a,7a) = −15 ppm, indicating that the hapticity of the ligand is best described as a distorted η^5-indenyl. This is in agreement with the crystallographic results.

X-ray crystal structure studies of $Rh(\eta^5\text{-}C_9H_7)(C_2H_4)_2$ (**9**) have recently been published.[13a,17] Some interesting comparisons can be made between **5** and **9**. The distance

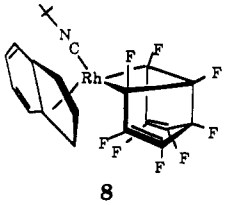

8

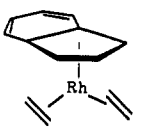

9

between the rhodium and the centroid of the indenyl ring is considerably longer in the C_8F_8 complex than in the ethylene complex (2.028 (3) Å vs 1.915 Å).[17] This would indicate that the indenyl ligand is more weakly bound in the fluorinated complex. Conversely, the average of the rhodium to olefinic carbon distance in **5** is shorter by approximately 0.05 Å than that in **9**, indicating a stronger metal–olefin bond in the perfluorinated case. The carbon-carbon bond distances in the indenyl ring are identical in the two complexes within experimental error. Thus it appears that in the solid state, the fluoroolefins in **5** are more tightly bound to the metal center than the olefins in **9**. The transfer of more electron density from the metal to the electron-deficient fluoroolefins appears to weaken the metal–indenyl bond, presumably due to decreased back-bonding to the indenyl ligand.

Table V. Comparison of the ^{19}F NMR Chemical Shift Data[a] for 1,2,5,6-η-OFCOT Complexes of Co and Rh

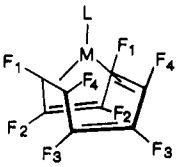

complex	$\delta(F_{2,3})$	$\delta(F_{1,4})$
2a: M = Co; L = C_5H_5	114.0	163.9
2b: M = Rh; L = C_5H_5	116.4	163.8
6a: M = Co; L = C_5Me_5	117.1	188.3
6b: M = Rh; L = C_5Me_2	118.3	187.3
5: M = Rh; L = C_9H_7	115.9	165.1

[a] Ppm upfield from internal $CFCl_3$; ambient temperature.

A comparison of the ^{19}F NMR spectral data for **5** with previously synthesized metal complexes of OFCOT (**2a, 2b, 6a, 6b**) (Table V) indicates that the assignment of 1,2,5,6-η-coordination of the C_8F_8 ring in these complexes is correct. All the complexes show two sets of fluorine resonances of equal intensity, one at approximately 117 ppm for the fluorines attached to the uncoordinated carbons and one at 160–190 ppm for the fluorines attached to the coordinated carbons. Again, the fluorines attached to coordinated carbons show the largest variation in chemical shift upon coordination to different metal centers.

If the solid-state structure of **5** is rigidly maintained in solution, one would expect four resonances of equal intensity in the ^{19}F NMR spectrum due to a plane of symmetry bisecting the coordinated C=C bonds of the C_8F_8 ring. Observation of only two resonances [δ 115.9 ($F_{2,3}$), 165.1 ($F_{1,4}$)] at room temperature indicated rapid rotation of the indenyl ring about the metal–indenyl axis on the NMR time scale. Variable-temperature ^{19}F NMR spectroscopic studies were undertaken to determine the barrier to this rotation.[12c,13,17] At −90 °C, the limiting spectrum was reached and the ^{19}F NMR spectrum showed four resonances [δ 118.2, 120.4, 164.2, 174.5] as would be expected from the solid-state structure. The resonances at δ 118.2 and 120.4 can be assigned to the fluorines attached to the uncoordinated carbons (F_2 and F_3) by comparison with the ^{19}F NMR chemical shift of free OFCOT (δ 123.2).[4] The resonance at δ 120.4 can be assigned to the fluorines attached to the uncoordinated carbon closest to the benzene ring (F_2) since these fluorines should experience the greater shielding due to the arene ring current. The other two resonances (δ 164.2, 174.5) can be assigned to the fluorines attached to the coordinated carbons (F_1, F_4) with the resonance at δ 174.5 assigned to F_1 by using the same criterion as above.

Computer simulation of the variable-temperature spectra by a line-shape analysis program of Binsch and Kleier[18] produced an E_a of 8.0 ± 0.6 kcal/mol for indenyl

(17) Mlekuz, M.; Bougeard, P.; Sayer, B. G.; McClinchey, M. J.; Rodger, C. A.; Churchill, M. R.; Ziller, J. W.; Kang, S.-K.; Albright, T. A. *Organometallics* **1986**, *5*, 1656–1663.

rotation. Using the Arrhenius equation, the ΔG^*_{190K} for indenyl rotation was calculated to be 8.6 ± 0.8 kcal/mol. The value of ΔG^*_{190K} for indenyl rotation in Rh(η-1-$CH_3C_9H_6$)(C_2H_4)$_2$ has been calculated to be 8.5 ± 0.4 kcal/mol.[17]

A more meaningful comparison of indenyl rotation is available from the cyclooctatetraene (COT) analogue of **5**.[8] Reaction of Rh(η^5-C_9H_7)(C_2H_4)$_2$ (**9**) with COT in refluxing hexane yielded the known complex **10** and the dinuclear complex **11**. This type of dinuclear structure is known for cyclopentadienyl and pentamethylcyclopentadienyl analogues of **11**.[19,20] A report of the synthesis of **11** by a different route has appeared recently together with a crystal structure study of the cyclopentadienyl analogue of **11**.[20]

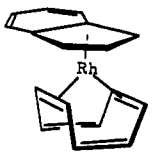

10

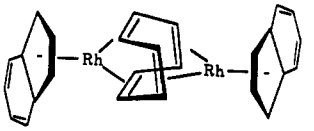

11

The yellow mononuclear complex **10** exhibited two resonances for the COT ligand in the ^{1}H NMR spectrum at room temperature.[8] A variable-temperature ^{1}H NMR study at 300 MHz in acetone-d_6 down to −90 °C showed no broadening of the COT resonances. Use of Freon 22 ($CHClF_2$, bp −44 °C) as a solvent (with a small amount of acetone-d_6 added as a lock solvent) allowed solution spectra to be obtained from −90 to −140 °C. At −140 °C, the limiting spectrum was reached and showed four resonances for the COT protons (3.90, 4.40, 5.37, 5.71 ppm). Lineshape analysis as described above produced an E_a for indenyl rotation of 9.4 ± 0.7 kcal/mol, which is not significantly different from the Rh(η^5-C_9H_7)(C_8F_8) results (8.0 ± 0.6 kcal/mol) described above.

Thus the indenyl rotation barriers do not appear to represent a satisfactory means of distinguishing differences in the slip-fold distortions of these two compounds.

Synthesis and Structural Studies of Dinuclear Indenyl Rhodium Complexes of OFCOT. Reaction of 2 equiv of Rh(η^5-C_9H_7)(C_2H_4)$_2$ with OFCOT yielded, in addition to **5**, a red, hexane-insoluble complex. The ^{19}F NMR spectrum of this red complex at room temperature showed four broad resonances, possibly indicating some type of fluxional behavior. Its ^{1}H NMR spectrum indicated two sets of indenyl resonances, and microanalysis results were consistent with a molecular formula of [$Rh_2(C_9H_7)_2(C_8F_8)$]. Single crystals were subjected to an X-ray diffraction study. The solid-state molecular structure was found to be **12**, and an ORTEP is shown in Figure 2. Details of the crystallographic determination are shown in Table VI. Fractional atomic coordinates are listed in Table VII, and selected bond angles and bond lengths are shown in Table VIII.

The compound contains a dinuclear core with a Rh(1)–Rh(2) distance of 2.719 (1) Å. The OFCOT ligand

Table VI. Crystallographic Data for Complexes 12 and 21

	(η^5-In)$_2$$Rh_2$-($C_8F_7H$) (**21**)	(η^5-In)$_2$$Rh_2$($C_8F_8$) (**12**)
formula	$C_{26}H_{15}F_7Rh_2$	$C_{26}H_{14}F_8Rh_2$
cryst system	monoclinic	monoclinic
space group	$P2_1/n$	$P2_1/c$
a, Å	11.375 (3)	8.170 (1)
b, Å	14.277 (3)	13.770 (1)
c, Å	14.211 (3)	20.079 (3)
β, deg	104.55 (2)	96.22 (1)
V, Å	2233.8 (9)	2245.6 (5)
Z	4	4
D(calcd), g cm^{-3}	1.970	2.013
μ(Mo Kα), cm^{-1}	14.97	14.98
color	deep red	deep red
size, mm	0.32 × 0.33 × 0.36	0.19 × 0.25 × 0.40
temp, K	292	293
T_{max}/T_{min}	0.706/0.624	0.693/0.577
diffractometer	Nicolet R3m/μ	Nicolet R3m/μ
radiatn	Mo Kα	Mo Kα
wavelength, Å	0.710 73	0.710 73
monochromator	graphite	graphite
scan method	ω	ω
scan limits, deg	$4 \le 2\theta \le 52$	$4 \le 2\theta \le 52$
data collected	$\pm h,+k,+l$	$\pm h,+k,+l$
rflns collected	4768	4509
indpdt reflns	4388	4201
R(int), %	2.08	2.45
obsd reflns ($\ge 4\sigma(F_o)$)	3533	3268
$R(F)$, $R(wF)$, %	3.22, 3.93	5.28, 6.57
GOF	1.153	1.866
Δ/σ	0.071	0.032
$\Delta(\rho)$, e Å^{-3}	0.71	1.16
N_o/N_v	11.0	9.9

Table VII. Atomic Coordinates (×10^4) and Isotropic Thermal Parameters (Å^2 × 10^3) for Complex 12

	x	y	z	U^a
Rh(1)	8117.5 (7)	8006.5 (4)	8618.0 (3)	42.5 (2)
Rh(2)	7160.1 (7)	6133.7 (5)	8759.1 (3)	39.8 (2)
Rh(2′)	7742 (6)	6110 (4)	8465 (3)	35 (2)
F(1)	3708 (7)	5561 (4)	8848 (3)	82 (2)
F(2)	2762 (8)	5892 (5)	7490 (4)	95 (3)
F(3)	5337 (10)	5970 (5)	6730 (3)	91 (3)
F(4)	8492 (7)	5835 (4)	7483 (3)	75 (2)
F(5)	8230 (8)	7708 (5)	7139 (3)	90 (2)
F(6)	5838 (9)	8841 (3)	7482 (3)	85 (2)
F(7)	4588 (7)	8712 (4)	8623 (3)	79 (2)
F(8)	4667 (7)	7215 (5)	9407 (3)	82 (2)
C(1)	4636 (11)	6154 (6)	8480 (5)	61 (3)
C(2)	4374 (10)	6002 (6)	7777 (5)	56 (3)
C(3)	5577 (14)	6014 (6)	7410 (4)	60 (3)
C(4)	7201 (11)	6329 (7)	7722 (4)	58 (3)
C(5)	7438 (10)	7406 (7)	7667 (4)	56 (3)
C(6)	6207 (10)	8043 (5)	7842 (4)	48 (2)
C(7)	5511 (9)	7929 (6)	8455 (4)	51 (3)
C(8)	5185 (10)	7025 (7)	8777 (4)	56 (3)
C(11)	7518 (12)	4598 (7)	9303 (4)	61 (3)
C(12)	8790 (11)	4715 (7)	8889 (5)	60 (3)
C(13)	9671 (11)	5605 (8)	9106 (5)	70 (3)
C(14)	8874 (13)	5936 (8)	9660 (5)	74 (4)
C(15)	7552 (15)	5390 (8)	9768 (5)	80 (4)
C(16)	6472 (13)	3757 (9)	9222 (7)	89 (5)
C(17)	6843 (16)	3093 (8)	8731 (7)	62 (5)
C(18)	8130 (19)	3270 (9)	8370 (7)	102 (5)
C(19)	9063 (17)	4015 (8)	8413 (6)	89 (5)
C(21)	9573 (10)	8564 (7)	9619 (4)	58 (3)
C(22)	8723 (10)	9337 (7)	9297 (5)	63 (3)
C(23)	9343 (14)	9422 (8)	8637 (5)	77 (4)
C(24)	10559 (13)	8740 (9)	8615 (5)	78 (4)
C(25)	10631 (11)	8172 (8)	9170 (5)	68 (3)
C(26)	9302 (16)	8298 (10)	10295 (5)	87 (4)
C(27)	8197 (18)	8861 (10)	10594 (6)	106 (6)
C(28)	7315 (15)	9602 (12)	10248 (7)	103 (6)
C(29)	7538 (14)	9885 (9)	9614 (7)	101 (5)

[a] Equivalent isotropic U defined as one-third of the trace of the orthogonalized U_{ij} tensor.

(18) The original version was written by: Kleier, D. A.; Binsch, G. *J. Magn. Reson.* **1970**, *3*, 146–160; Program 165, Quantum Chemistry Program Exchange, Indiana University. Modifications are described in: Bushweller, C. H.; Bhat, G.; Lentendre, L. J.; Brunelle, J. A.; Bilofsky, H. S.; Ruben, H.; Templeton, D. H.; Zalkin, A. *J. Am. Chem. Soc.* **1975**, *97*, 65–73.

(19) Lauher, J. W.; Elian, M.; Summerville, R. H.; Hoffmann, R. *J. Am. Chem. Soc.* **1976**, *98*, 3219–3224.

(20) Bieri, J. H.; Egolf, T.; von Philipsborn, W.; Piantini, U.; Prewo, R.; Ruppli, U.; Salzer, A. *Organometallics* **1986**, *5*, 2413–2425.

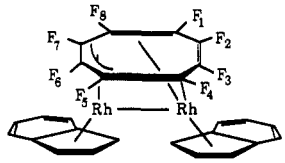

12

spans the metal–metal bond with Rh(1) bound to C(5), C(6), C(7) in an η^3-allyl fashion and Rh(2) bound to C(4) in a η^1-fashion and to C(1) and C(8) in a η^2-fashion. As expected, the coordinated C=C bond is substantially lenghtened upon coordination [C(1)—C(8) = 1.39(1) Å vs C(2)—C(3) = 1.29 (1) Å].

This type of bonding has been observed previously in dinuclear metal complexes of substituted and unsubstituted 1,3,5-cyclooctatrienes (**13–15**)[21–23] and in dinuclear ruthenium (**16**)[24] and rhodium (**17**)[20] complexes of cyclooctatetraene. The closest analogue of **12** is the structurally

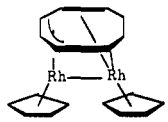

13

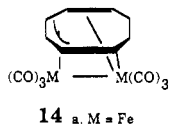

14 a. M = Fe
b. M = Ru

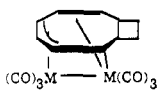

15 a. M = Fe
b. M = Ru

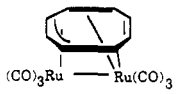

16

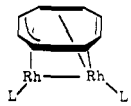

17 a. L = Cp
b. L = Cp*

characterized complex **17a**[20] which provides a useful structural comparison to **12**. One notable difference is the shortened metal–olefin bond distance in **12** [**17a**, Rh–CH_{olefin} (average) = 2.128 Å; **12**, Rh–CF_{olefin} (average) = 2.054 (8) Å]. This can be attributed to increased backbonding from the metal center to the electron-deficient olefin as discussed previously. Depletion of electron density at the metal center also leads apparently to a weakening of the metal–metal bond as evidenced by the longer Rh–Rh distance in the fluorinated complex [**12**, Rh(1)–Rh(2) = 2.719 (1) Å; **17a**, Rh–Rh = 2.689 (1) Å].

Spectroscopic Studies of Stereochemical Nonrigidity of the OFCOT Ligand in Complex 12. If the solid-state structure of **12** were rigidly maintained in solution, the ^{19}F NMR spectrum should show eight resonances due to symmetry inequivalent fluorines. However, only four broad resonances were present in the ^{19}F NMR spectrum at room temperature, indicative of a fluxional process. It was anticipated that the nature of this dynamic behavior might be analogous to that observed for similar dinuclear complexes of COT or 1,3,5-cyclooctatriene.[20–23] This process involves the conversion of the two enantiomorphs of **12**. Two mechanisms have been proposed for this interconversion; a "glide" (Scheme I) and a "twitch" (Scheme II).[22]

At the low-temperature limit in both mechanisms, there should be eight resonances in the ^{19}F NMR spectrum and

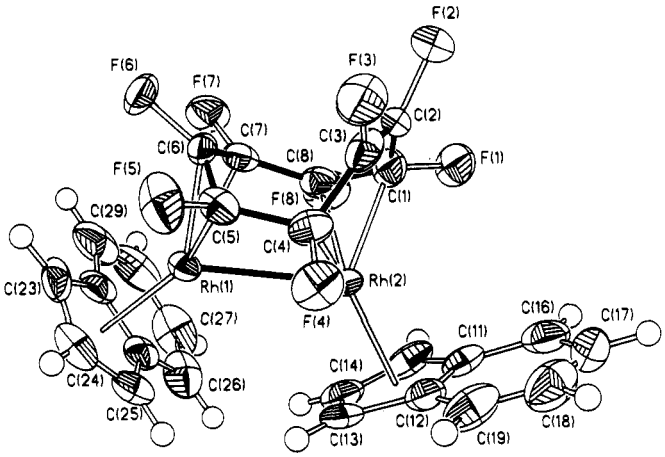

Figure 2. Molecular structure and atom labeling scheme for complex **12**.

Scheme I. "Glide" Mechnism for Site Exchange in Complex 12

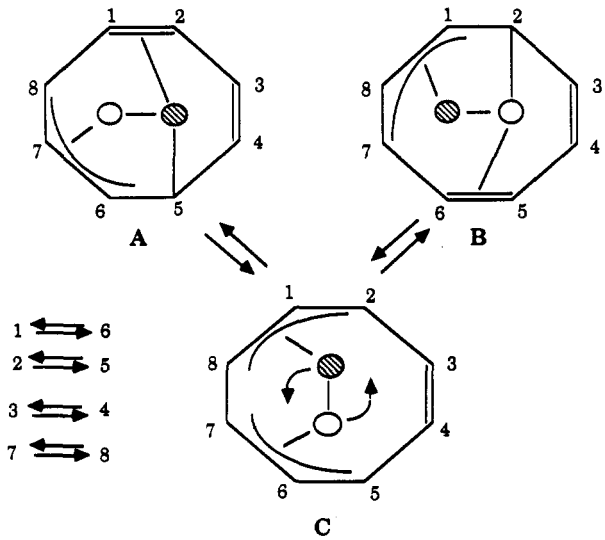

Scheme II. "Twitch" Mechanism for Site Exchange in Complex 12

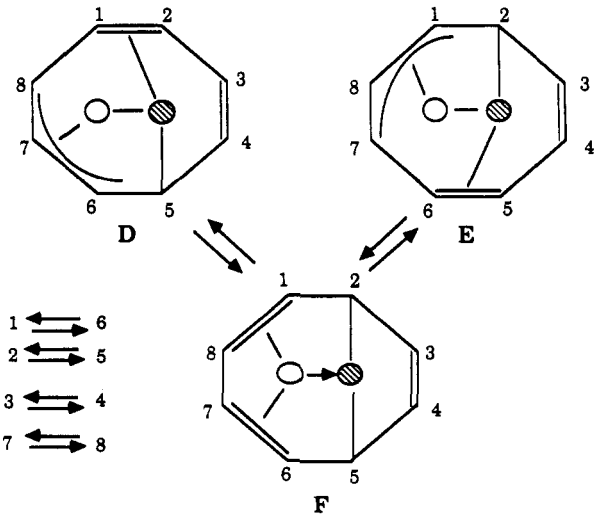

two sets of indenyl resonances in the ^1H NMR spectrum if the solution structure is analogous to that in the solid state. If the glide mechanism were operative here, the ^{19}F NMR spectrum at high temperatures should show four sets of fluorine resonances due to the rapid exchange of F_1 with F_6, F_2 with F_5, F_3 with F_4, and F_7 with F_8 (see Scheme I).

(21) Evans, J.; Johnson, B. F. G.; Lewis, J.; Watt, R. *J. Chem. Soc., Dalton Trans.* **1974**, 2368–2374.
(22) Deganello, G.; Lewis, J.; Parker, D. G.; Sandrin, P. L. *Inorg. Chim. Acta* **1977**, *24*, 165–171.
(23) Szary, A. C.; Knox, S. A. R.; Stone, F. G. A. *J. Chem. Soc., Dalton Trans.* **1974**, 662–664.
(24) (a) Cotton, F. A.; Davison, A.; Marks, T. J.; Musco, A. *J. Am. Chem. Soc.* **1969**, *91*, 9598–6603. (b) Cotton, F. A.; Edwards, W. T. *J. Am. Chem. Soc.* **1968**, *90*, 5412–5417.

Table VIII. Selected Bond Distances and Angles for Complexes 12 and 21[a]

	$(\eta^5\text{-In})_2Rh_2(C_8F_7H)$ (21)	$(\eta^2\text{-In})_1Rh_2(C_8F_8)$ (12)
	(a) Bond Distances (Å)	
Rh(1)–Rh(2)	2.713 (1)	2.719 (1)
Rh(1)–CNT(1)	1.925 (3)	1.925 (7)
Rh(2)–CNT(2)	1.936 (3)	1.939 (7)
Rh(1)–C(5)	2.092 (4)	2.099 (8)
Rh(1)–C(6)	2.074 (4)	2.083 (8)
Rh(1)–C(7)	2.117 (4)	2.122 (7)
Rh(2)–C(4)	2.077 (4)	2.103 (9)
Rh(2)–C(1)	2.114 (4)	2.077 (9)
Rh(2)–C(8)	2.108 (4)	2.031 (8)
C(1)–C(2)	1.446 (6)	1.42 (1)
C(2)–C(3)	1.319 (6)	1.29 (1)
C(3)–C(4)	1.480 (6)	1.47 (1)
C(4)–C(5)	1.487 (6)	1.50 (1)
C(5)–C(6)	1.421 (6)	1.41 (1)
C(6)–C(7)	1.427 (6)	1.42 (1)
C(7)–C(8)	1.471 (6)	1.44 (1)
C(8)–C(1)	1.423 (6)	1.39 (1)
	(b) Bond Angles (deg)	
CNT(1)–Rh(1)–Rh(2)	135.2 (1)	135.7 (2)
CNT(2)–Rh(2)–Rh(1)	122.3 (1)	120.8 (2)
CNT(1)–Rh(1)–C(5)	137.9 (2)	140.0 (3)
CNT(1)–Rh(1)–C(6)	139.6 (2)	140.0 (3)
CNT(1)–Rh(1)–C(7)	139.6 (2)	137.9 (3)
CNT(2)–Rh(2)–C(4)	130.4 (2)	127.9 (3)
CNT(2)–Rh(2)–C(1)	128.1 (2)	130.0 (3)
CNT(2)–Rh(2)–C(8)	135.4 (2)	139.5 (3)
C(5)–Rh(1)–C(6)	39.9 (2)	34.9 (3)
C(5)–Rh(1)–C(7)	71.8 (2)	71.2 (3)
C(6)–Rh(1)–C(7)	39.8 (2)	39.4 (3)
C(4)–Rh(2)–C(1)	81.1 (2)	81.6 (4)
C(4)–Rh(2)–C(8)	93.4 (1)	92.2 (3)
C(1)–Rh(2)–C(8)	39.4 (2)	39.6 (3)
C(1)–C(2)–C(3)	119.7 (4)	121.6 (8)
C(2)–C(3)–C(4)	117.6 (4)	117.9 (8)
C(3)–C(4)–C(5)	111.7 (3)	112.2 (7)
C(4)–C(5)–C(6)	120.7 (4)	119.7 (7)
C(5)–C(6)–C(7)	120.2 (3)	120.8 (7)
C(6)–C(7)–C(8)	129.2 (4)	126.6 (7)
C(7)–C(8)–C(1)	125.2 (4)	128.2 (8)
C(8)–C(1)–C(2)	129.6 (4)	124.0 (8)

[a] CNT(1) = centroid of C(21), C(22), C(23), C(24), C(25). CNT(2) = centroid of C(11), C(12), C(13), C(14), C(15).

Also, only one set of indenyl resonances should be seen since the two rhodium centers also interconvert through a bis(allyl) species represented by C in Scheme I. If the twitch mechanism were operative, the high-temperature ^{19}F NMR spectrum should also show four sets of fluorine resonances due to the rapid exchange of F_1 with F_6, F_2 with F_5, F_3 with F_4, and F_7 and F_8 (see Scheme II). However, the two rhodium centers remain distinct and would not interconvert, leading to two sets of indenyl resonances.

Complex **12** was subjected to low-temperature ^1H and ^{19}F NMR spectroscopy studies in acetone-d_6 and high-temperature ^1H and ^{19}F NMR spectroscopy studies in toluene-d_8. At −40 °C, eight sharp fluorine resonances (δ 113.9, 125.7, 147.2, 154.7, 155.3, 172.8, 177.8, 188.9) and two sets of indenyl resonances were observed as expected (spectral assignments appear later in this section). At −93 °C, two sets of eight resonances (20:3 relative ratio) were seen in the ^{19}F NMR spectrum. As discussed previously, it is possible to slow indenyl rotation on the NMR time scale at low temperatures. At −40 °C, it seems that indenyl rotation is still fast, but the fluxional process of the C_8F_8 ring has slowed, explaining the single set of eight resonances. However, at −93 °C, the indenyl rotation may have slowed sufficiently to allow observation of a second isomer in which the indenyl ligands are in a different conformation with respect to each other.

At 90 °C, there were four sets of fluorine resonances and two sets of indenyl resonances. This indicated that the glide mechanism is not operative here and the twitch mechanism is probably responsible for the interconversion of the enantiomorphs of **12**. The twitch mechanism also seems to be operative in all of the reported cis dinuclear COT and 1,3,5-cyclooctatriene complexes.[21-23] Structures with this type of dynamic behavior (e.g. **17a**) were also characterized by two inequivalent ^{103}Rh NMR resonances.[20] Line-shape analysis of the variable-temperature ^{19}F NMR spectra of **12** yielded an E_a of 16.3 ± 0.4 kcal/mol and a $\Delta G^{\ddagger}_{247K}$ of 13.7 ± 0.4 kcal/mol.[25] While E_a's were not calculated for the fluxional processes of **13–17**,[21-23] the complex that allows for the most direct comparison of $\Delta G^{\ddagger}$ values is **13** ($\Delta G^{\ddagger}_{247K}$ = 12.9 kcal/mol).[21] Although no uncertainties were reported for the calculation of $\Delta G^{\ddagger}$ for **13**, it appears that perfluorination does not appreciably effect the activation barrier for stereochemical nonrigidity in these dinuclear rhodium complexes.

The ^{19}F NMR spectral assignments for **12** can be made on the basis of chemical shift values at −40 °C and variable-temperature ^{19}F NMR data. By observing which resonances coalesce upon warming from −40 to +90 °C, it is possible to distinguish which pairs of fluorines are exchanging (see Scheme II). The resonances at δ 113.9 and 125.7 coalesce and can be assigned to F_2 and F_3 on the basis of comparison with the ^{19}F NMR chemical shift of free OFCOT (δ 123.2)[4] and assignments made on the 1,2,3,6-η isomer of $[Rh(\eta\text{-}C_5Me_5)(C_8F_8)]$ (**7b**).[6] The resonances at δ 154.7 and 155.3 coalesce and can be assigned to F_6 and F_7 since these two fluorines should be most similar in chemical shift. The resonances at δ 177.8 and 188.9 coalesce and can be assigned to F_1 and F_4. The chemical shift of F_4 would be expected to be further upfield since it is attached to a carbon directly bound to a metal center. The resonances at δ 147.2 and 172.8 coalesce and can be assigned to F_5 and F_8.

Mechanism of Formation of Dinuclear Rhodium OFCOT Complexes from the Mononuclear Complex 5. Reaction of 1 equiv of the isolated mononuclear species **5** with 1 equiv of $Rh(\eta^5\text{-}C_9H_7)(C_2H_4)_2$ led to clean formation of the dinuclear species **12** presumably via an intermediate in which both rhodiums are coordinated to the same side of the perfluorinated ring. This cis coordination in the intermediate is necessary since no trans product analogous to **11** was observed in the reaction. Since this intermediate was not observable under the reaction conditions, it was hoped that the addition of exogenous ligands to the dinuclear species would lead to complexes having the same structural properties as the intermediate.

A color change from deep red to yellow was noticed when carbon monoxide was bubbled through a solution of **12** in THF. A ^{19}F NMR spectrum taken at this point showed two sets of four resonances: one set due to the major component (δ 111.3, 119.9, 138.2, 169.2) and a second set due to the minor component (δ 117.2, 118.8, 135.5, 176.3). Additionally, there were two carbonyl absorbances in the IR spectrum. It would appear, based on this spectroscopic data, that there were two isomers present, and the bonding of the C_8F_8 ring to the metals was the same in each isomer. Removal of the solvent followed by crystallization of the residue from methylene chloride/hexane at −20 °C led to yellow single crystals of the major isomer as identified by ^{19}F NMR spectroscopy. The molecular structure of this complex (**18**) is shown in Figure 3. Details of the crystallographic determination are listed in Table IX, frac-

(25) Martin, M. L.; Martin, J. L.; Delpeuch, J.-J. *Practical NMR Spectroscopy*; Heyden: Philadelphia, 1980; Chapter 8, p 339.

Table IX. Crystallographic Parameters for Complex 18

(a) Crystal Parameters			
formula	$C_{27}H_{17}F_8ORh_2$	γ, deg	97.63 (2)
cryst system	triclinic	V, Å^{-3}	1187.2 (4)
space group	$P\bar{1}$	Z	2
a, Å	8.947 (1)	μ, cm^{-1}	14.3
b, Å	9.840 (3)	D(calcd), g cm^{-3}	2.000
c, Å	14.081 (3)		
α, deg	96.94 (2)	temp, K	293
β, deg	102.11	color	yellow
		size, mm	0.32 × 0.34 × 0.35
(b) Data Collection			
diffractometer	Nicolet R3m/μ	rflns collected	5415
		indepdt rflns	4658
radiatn	Mo Kα	obsd rflns ($4\sigma(F_o)$)	4184
wavelength, Å	0.710 73		
monochromator	graphite	R(int), %	0.69
		std rflns	3 std/197 rflns
2θ limits, deg	$4 \le 2\theta \le 52$		
scan method	ω	decay	<1%
(c) Refinement			
$R(F)$, %	2.06	Δ/σ(max)	0.05
$R(wF)$, %	2.80	$\Delta(\rho)$, e Å^{-3}	0.40
GOF	0.69	N_o/N_v	12.2

Table X. Atomic Coordinates (×10^4) and Isotropic Thermal Parameters (Å^2 × 10^3) for Complex 18

	x	y	z	U^a
Rh(1)	2211.2 (2)	2145.0 (2)	838.6 (1)	28.2 (1)
Rh(2)	2287.8 (2)	2058.8 (2)	3758.2 (1)	27.8 (1)
F(1)	1126 (2)	−938 (2)	3681 (1)	54 (1)
F(2)	3928 (3)	−1718 (2)	3422 (2)	61 (1)
F(3)	6407 (2)	416 (2)	3968 (2)	59 (1)
F(4)	5625 (2)	2949 (2)	4668 (1)	47 (1)
F(5)	4535 (2)	4057 (2)	3099 (1)	39 (1)
F(6)	5244 (2)	1563 (2)	1864 (1)	42 (1)
F(7)	2835 (2)	−549 (2)	1358 (1)	43 (1)
F(8)	26 (2)	183 (2)	2109 (1)	48 (1)
O	3580 (4)	584 (3)	−656 (2)	80 (1)
C(1)	2154 (3)	−60 (3)	3350 (2)	37 (1)
C(2)	3743 (4)	−375 (3)	3585 (2)	41 (1)
C(3)	4920 (3)	639 (3)	3839 (2)	39 (1)
C(4)	4640 (3)	2074 (3)	3892 (2)	34 (1)
C(5)	4060 (3)	2658 (2)	3034 (2)	28 (1)
C(6)	3839 (3)	1841 (3)	2051 (2)	28 (1)
C(7)	2553 (3)	723 (2)	1781 (2)	30 (1)
C(8)	1588 (3)	525 (3)	2497 (2)	33 (1)
C(9)	3110 (4)	1150 (3)	−71 (2)	43 (1)
C(11)	1265 (3)	4121 (3)	4305 (2)	35 (1)
C(12)	13 (3)	2998 (3)	4039 (2)	37 (1)
C(13)	452 (4)	1908 (3)	4587 (2)	44 (1)
C(14)	1892 (4)	2418 (3)	5248 (2)	48 (1)
C(15)	2471 (4)	3706 (3)	5012 (2)	43 (1)
C(16)	1133 (4)	5359 (3)	3912 (2)	41 (1)
C(17)	−238 (4)	5465 (3)	3308 (2)	44 (1)
C(18)	−1474 (4)	4347 (4)	3037 (2)	46 (1)
C(19)	−1359 (3)	3119 (3)	3372 (2)	43 (1)
C(21)	1777 (3)	4463 (3)	1061 (2)	38 (1)
C(22)	1546 (3)	4011 (3)	34 (2)	39 (1)
C(23)	341 (4)	2804 (3)	−227 (2)	47 (1)
C(24)	−205 (3)	2576 (3)	605 (3)	49 (1)
C(25)	761 (3)	3479 (3)	1426 (2)	42 (1)
C(26)	2869 (4)	5644 (3)	1517 (3)	51 (1)
C(27)	3675 (4)	6338 (4)	948 (3)	65 (1)
C(28)	3465 (4)	5890 (4)	−60 (3)	67 (2)
C(29)	2424 (4)	4733 (4)	−516 (3)	55 (1)

[a] Equivalent isotropic U defined as one-third of the trace of the orthogonalized U_{ij} tensor.

tional atomic coordinates are presented in Table X, and selected bond angles and bond lengths are shown in Table XI.

Both rhodiums are still coordinated in a cis fashion to the C_8F_8 ring, but there is no longer a Rh–Rh bond. Rh(2) is bound in a 1,2,5,6-η fashion to the perfluorinated ring, while Rh(1) is bound in an η^2-fashion to an olefinic bond of the ring and to the added CO ligand. This structure nicely models what the intermediate in the formation of the dinuclear species might look like structurally, i.e. resulting from attack of a coordinatively unsaturated Rh(C_9H_7)L fragment on the less hindered exo face of one of the uncoordinated fluoroolefins of **5**. Loss of CO and formation of a metal–metal bond followed by or in conjunction with rearrangement of the bonding to the C_8F_8 ring would lead to **12**. In agreement with this hypothesis, heating a solution of **18** indeed led to dissociation of the CO ligand and formation of **12** as evidenced by ^{19}F NMR spectroscopy. It seems quite reasonable that formation of cis dinuclear structures such as **12** and its hydrocarbon relatives occurs by such a stepwise process. Notably formation of the trans dinuclear complex **11** from **10** should be less favorable, since it would involve attack on the more hindered endo face of an uncoordinated olefin of **10**; the

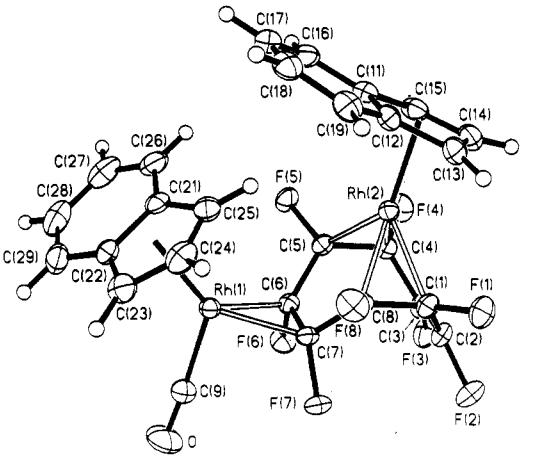

Figure 3. Molecular structure and atom labeling scheme for complex **18**.

Table XI. Selected Bond Distances and Angles for Complex 18[a]

(a) Bond Distances (Å)			
Rh(1)–CNT(1)	1.916 (3)	Rh(2)–C(11)	2.441 (3)
Rh(2)–CNT(2)	1.954 (3)	Rh(2)–C(12)	2.429 (3)
Rh(1)–C(6)	2.079 (2)	Rh(2)–C(13)	2.206 (3)
Rh(1)–C(7)	2.050 (3)	Rh(2)–C(14)	2.195 (3)
Rh(1)–C(9)	1.894 (3)	Rh(2)–C(15)	2.211 (3)
Rh(2)–C(1)	2.076 (3)	C(1)–C(2)	1.473 (4)
Rh(2)–C(4)	2.071 (3)	C(2)–C(3)	1.308 (4)
Rh(2)–C(5)	2.117 (3)	C(3)–C(4)	1.463 (4)
Rh(2)–C(8)	2.112 (3)	C(4)–C(5)	1.429 (4)
Rh(1)–C(21)	2.359 (3)	C(5)–C(6)	1.475 (3)
Rh(1)–C(22)	2.349 (3)	C(6)–C(7)	1.434 (3)
Rh(1)–C(23)	2.223 (3)	C(7)–C(8)	1.472 (4)
Rh(1)–C(24)	2.223 (3)	C(8)–C(1)	1.422 (4)
Rh(1)–C(25)	2.175 (3)	C(9)–O	1.123 (5)
(b) Bond Angles (deg)			
CNT(1)–Rh(1)–C(6)	135.2 (1)	C(1)–Rh(2)–C(8)	39.7 (1)
CNT(1)–Rh(1)–C(7)	136.8 (1)	C(4)–Rh(2)–C(5)	39.9 (1)
CNT(1)–Rh(1)–C(9)	127.3 (1)	C(4)–Rh(2)–C(8)	95.3 (1)
C(6)–Rh(1)–C(7)	40.6 (1)	C(5)–Rh(2)–C(8)	81.1 (1)
C(6)–Rh(1)–C(9)	93.5 (1)	C(1)–C(2)–C(3)	119.7 (3)
C(7)–Rh(1)–C(9)	91.4 (1)	C(2)–C(3)–C(4)	119.4 (3)
Rh(1)–C(9)–O	175.7 (3)	C(3)–C(4)–C(5)	122.2 (2)
CNT(2)–Rh(2)–C(1)	128.9 (1)	C(4)–C(5)–C(6)	119.9 (2)
CNT(2)–Rh(2)–C(4)	129.3 (1)	C(5)–C(6)–C(7)	115.6 (2)
CNT(2)–Rh(2)–C(5)	135.1 (1)	C(6)–C(7)–C(8)	117.3 (2)
CNT(2)–Rh(2)–C(8)	135.0 (1)	C(7)–C(8)–C(1)	119.9 (2)
C(1)–Rh(1)–C(4)	83.3 (1)	C(8)–C(1)–C(2)	121.7 (3)
C(1)–Rh(2)–C(5)	95.7 (1)		

[a] CNT(1) = centroid of C(21), C(22), C(23), C(24), C(25). CNT(2) = centroid of C(11), C(12), C(13), C(14), C(15).

fact that **11** is indeed formed is surprising, therefore.

Presumably, the structure of the minor isomer observed spectroscopically in the reaction of **12** with carbon monoxide is an isomer of the crystallographically characterized complex **18**. Rotation about the Rh(1)–olefin axis would lead to a complex in which the carbon monoxide ligand is now directed toward the indenyl ligand attached to Rh(2) as shown in **19**.

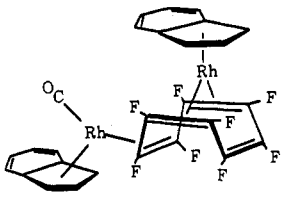

19

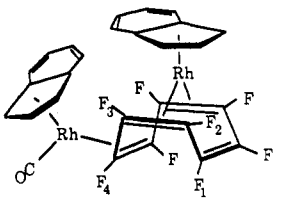

18

The ^{19}F NMR spectral assignments of **18** were made by a comparison of shift values for known complexes and variable-temperature studies. The resonance at δ 119.9 can be assigned to the fluorines attached to the uncoordinated carbon (F_1) by comparison with the ^{19}F NMR chemical shift of free OFCOT (δ 123.2).[4] The resonance at δ 169.2 can be assigned to F_2 by comparison with the chemical shift of the fluorines attached to coordinated carbons in 1,2,5,6-η complexes (δ 160–190). The resonance at δ 111.3 can be assigned to F_4 by comparison of the chemical shift of the fluorines attached to the coordinated carbons in the 1,2-η iron complex of C_8F_8 (δ 97.0).[26] The resonance at δ 138.2 can then be assigned to F_3. Identification of the ^{19}F–^{19}F coupling constants for this complex supports these assignments: F_1 is coupled to F_2 (J = 28 Hz); F_2 is coupled to F_1 and F_3 (J = 28 Hz); and F_3 is coupled to F_2 and F_4 (J = 28 Hz).

As a final confirmation of these assignments, variable-temperature ^{19}F NMR spectroscopic studies were performed on **18**. As discussed above, indenyl rotation on the NMR time scale can be slowed at temperatures as high as –60 °C. A solution of **18** in toluene-d_8 was cooled to –93 °C, and ^{19}F NMR spectra were recorded at various temperatures as the solution was warmed. Two resonances, one at δ 117.4 and a second at δ 107.5, coalesced slowly to give a resonance at δ 111.3 at room temperature. The resonance at δ 119.9 remained sharp throughout the low-temperature studies. A broad resonance at δ 138.2 and a slightly broader resonance at δ 170 sharpened quickly to give the resonances at δ 138.2 and 169.2 at room temperature.

This variable-temperature behavior supports the proposed ^{19}F NMR spectral assignments. The resonance at δ 119.9 had been assigned to the free olefin fluorines (F_1) which would be least influenced by indenyl rotation. The resonances of the fluorines attached to the olefins coordinated to Rh(2) (F_2, F_3) should broaden at similar rates. The fluorines attached to the olefin coordinated to Rh(1) (F_4) would be most influenced by the indenyl rotation and would have very different chemical shifts when the indenyl rotation was slowed.

Attempts to add ethylene to **12** in hopes of obtaining the actual intermediate were only partially successful. Spectroscopically, it appeared that the product **20** of this reaction was structurally akin to **18**, but ethylene rapidly dissociated in solution even at –20 °C to give **12**, making crystallization of a clean product very difficult. However, it is clear that a complex such as **20** is the most likely intermediate in the formation of the dinuclear species **12**.

Table XII. Atomic Coordinates (×10⁴) and Isotropic Thermal Parameters (Å² × 10³) for Complex 21

	x	y	z	U^a
Rh(1)	3897.2 (3)	328.2 (3)	2228.0 (2)	44 (1)
Rh(2)	1705.1 (3)	448.2 (2)	2651.2 (2)	43 (1)
F(1)	1173 (3)	-357 (2)	4430 (2)	75 (1)
F(2)	2429 (3)	1015 (2)	5646 (2)	72 (1)
F(3)	2996 (3)	2571 (2)	4702 (2)	74 (1)
F(4)	2210 (2)	2462 (2)	2644 (2)	68 (1)
F(5)	4629 (3)	2237 (2)	3066 (2)	79 (1)
F(6)	5801 (2)	815 (2)	4071 (2)	70 (1)
F(7)	4898 (2)	-877 (2)	3989 (2)	68 (1)
C(1)	2073 (4)	136 (3)	4151 (3)	52 (1)
C(2)	2343 (4)	1011 (3)	4673 (3)	54 (1)
C(3)	2569 (4)	1767 (3)	4213 (3)	50 (1)
C(4)	2655 (4)	1654 (3)	3197 (3)	46 (1)
C(5)	3926 (4)	1479 (3)	3145 (3)	48 (1)
C(6)	4604 (4)	722 (3)	3663 (3)	51 (1)
C(7)	4059 (4)	-179 (3)	3655 (3)	49 (1)
C(8)	2819 (4)	-422 (3)	3706 (3)	48 (1)
C(11)	-431 (4)	263 (3)	2260 (3)	61 (2)
C(12)	-166 (4)	1074 (4)	1773 (3)	57 (2)
C(13)	631 (4)	807 (5)	1186 (3)	83 (2)
C(14)	746 (5)	-153 (5)	1221 (4)	108 (3)
C(15)	179 (5)	-521 (4)	1915 (5)	95 (3)
C(16)	-1188 (5)	339 (5)	2900 (4)	83 (2)
C(17)	-1645 (5)	1172 (5)	3050 (4)	92 (3)
C(18)	-1405 (4)	1956 (4)	2581 (4)	83 (2)
C(19)	-663 (4)	1964 (4)	1951 (4)	71 (2)
C(21)	3641 (4)	477 (3)	552 (3)	56 (2)
C(22)	4812 (4)	820 (4)	1030 (3)	61 (2)
C(23)	5456 (5)	63 (5)	1610 (4)	90 (2)
C(24)	4713 (6)	-730 (4)	1412 (4)	98 (3)
C(25)	3596 (6)	-490 (4)	827 (4)	80 (2)
C(26)	2810 (5)	1067 (6)	-66 (4)	103 (3)
C(27)	3134 (8)	1958 (6)	-181 (5)	140 (4)
C(28)	4265 (8)	2296 (4)	292 (5)	140 (5)
C(29)	5133 (7)	1750 (4)	886 (4)	98 (3)

[a] Equivalent isotropic U defined as one-third of the trace of the orthogonalized U_{ij} tensor.

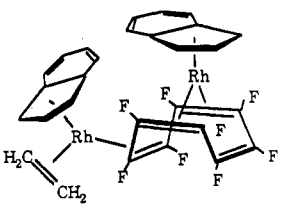

20

Reaction of 12 with Chromatography Supports. During the course of this work, the purification of **12** was attempted via column chromatography on silica gel. Instead of purifying **12**, a reaction on the column support occurred to produce a new complex. At room temperature, this complex exhibited seven sharp resonances in the ^{19}F NMR spectrum (δ 116, 125, 140, 147, 154, 180, 185) and two sets of indenyl resonances in the ^1H NMR spectrum together with an additional ^1H NMR resonance at δ 4.6. Single crystals of this complex (**21**) were produced from

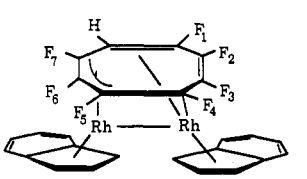

21

(26) Barefoot, A. C., III; Corcoran, E. W., Jr.; Hughes, R. P.; Lemal, D. M.; Saunders, W. D.; Laird, B. B.; Davis, R. E. *J. Am. Chem. Soc.* **1981**, *103*, 970–972. The molecular structure of $Fe(CO)_4$(1,2-η-OFCOT) has been confirmed by a single-crystal X-ray diffraction study: Davis, R. E., private communication.

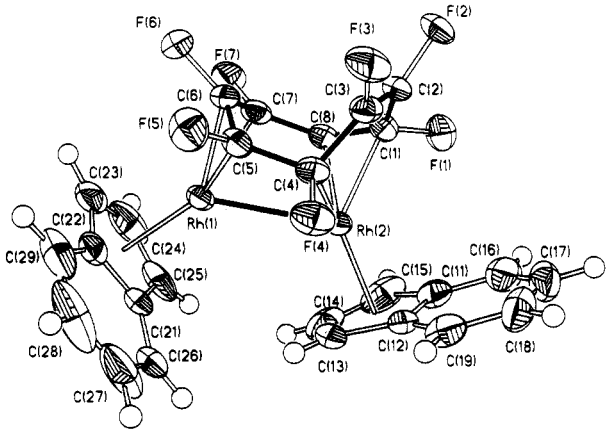

Figure 4. Molecular structure and atom labeling scheme for complex **21**.

methylene chloride/hexane at −20 °C and submitted for X-ray diffraction studies. The molecular structure of **21** is shown in Figure 4. Details of the crystallographic determination are shown in Table VI, fractional atomic coordinates are provided in Table XII, and selected bond angles and bond lengths are shown in Table VIII.

The ^{19}F NMR resonances were assigned as described above for **12**. The resonance at δ 172.8 that corresponded to F_8 in **12** is noticeably absent in the spectrum of **21**. Also, it is interesting to note that F_7 is shifted downfield by 15 ppm, presumably due to the decreased shielding upon replacement of an adjacent fluorine by a hydrogen.

Clearly, formation of **21** from **12** involves a selective fluorine–hydrogen exchange. This is remarkable since C–F bonds are considerably stronger than their C–H analogues. Presumably, a strong fluorine bond to another element must be formed to make up for the bond energy difference between the C–X bonds. It was originally anticipated that a strong Si–F bond might be formed on the silica gel but further investigation showed that the H–F exchange also occurred on alumina. The fate of the fluorine is unknown, as is the source of the hydrogen. It does not arise from the reaction of **12** with the solvents used in the chromatography since stirring **12** in each of the solvents did not produce **21** as evidenced by ^{19}F NMR spectroscopy. Attempts to produce **21** by addition of acids ($HBF_4 \cdot Et_2O$, CF_3COOH) to **12** did not lead to **21** or any other heptafluoro complexes as evidenced by ^{19}F NMR spectroscopy. Contact time on the column support also influenced production of **21**. Rapid chromatography over a span of 5 min allowed recovery of **12** unchanged while chromatography over a 3-h span led to formation of **21**.

Additional chromatography allowed for isolation of minor amounts of a second complex (**22**). Unfortunately, it could not be totally separated from the major isomer **21**, and, therefore, only spectroscopic data exist for this complex. The location of the lone hydrogen remains unknown but it appears to be a positional isomer of the major product. This isomer along with what appear to be other heptafluoro isomers can be produced by heating solutions of **21** up to 80 °C. Apparently scrambling of the single proton occurs around the ring to give a mixture of heptafluoro products, confirming that the initial production of the major isomer **21** was kinetically selective. The mechanism of this remarkable reaction is still unclear.

Complex **21** and the other isomers of this product are not fluxional on the NMR time scale as evidenced by seven sharp resonances in the ^{19}F NMR spectrum at room temperature. The replacement of a fluorine by a hydrogen presumably causes a thermodynamic preference for a single isomer.

Experimental Procedures

General Data. Infrared spectra were recorded on a Perkin-Elmer 257 or 599 dispersive infrared spectrophotometer, calibrated against the 1601 cm^{-1} peak of polystyrene, or on a Bio-Rad Digilab FTS-40 Fourier Transform infrared spectrophotometer. ^1H NMR spectra (300 MHz) were recorded on a Varian Associates XL-300 spectrometer at 25 °C unless otherwise noted. ^{19}F NMR spectra were recorded on a JEOL FX60Q spectrometer (56.20 MHz) or on a Varian Associates XL-300 spectrometer (282 MHz) at 25 °C unless otherwise noted. All ^{19}F shifts are reported in parts per million upfield from the internal standard of $CFCl_3$. All ^1H shifts are reported in parts per million downfield from tetramethylsilane. Variable-temperature NMR spectra were taken on a Varian Associates XL-300 spectrometer. The probe was calibrated at various temperatures by using samples of methanol (low temperature)[27] and ethylene glycol (high temperature).[28]

Melting points were determined using an Electrothermal capillary melting point apparatus and are uncorrected. Microanalyses were done at Atlantic Microlab, Inc., Atlanta, GA, or Spang Microanalytical Laboratory, Eagle Harbor, MI.

Organometallic reaction solvents, crystallization solvents, and chromatography solvents were dinitrogen-saturated and distilled over a variety of drying agents. Benzene and tetrahydrofuran were dried over potassium, toluene was dried over sodium, hexane and diethyl ether were dried over sodium-potassium alloy, and methylene chloride was dried over P_4O_{10}. All organometallic reactions were run in oven-dried glassware using conventional Schlenk techniques, under an atmosphere of dinitrogen which was deoxygenated over BASF catalyst and dried by using Aquasorb, or in a Vacuum Atmospheres drybox equipped with a HE-492 gas purification system. Column chromatography was done under dinitrogen in jacketed columns with dry, N_2-saturated chromatography supports and solvents. All deuteriated solvents were dried over P_4O_{10} and degassed prior to use.

Silica gel (Davisil 62, Activity III) was obtained from Davison Chemical, Inc. Alumina (Activity III) was obtained from ICN Pharmaceuticals, Inc. Rhodium(III) trichloride hydrate was obtained from Matthey Bishop, Inc.

1,3,5,7-Octafluorocyclooctatetraene (OFCOT) (**1**) was prepared according to the method of Lemal.[4] (η^5-Indenyl)bis(η-ethylene)rhodium(I) (**9**) was prepared according to the method of Green.[8]

Reaction of Rh(η^5-C_9H_7)(C_2H_4)$_2$(9) with OFCOT. Formation of (η^5-Indenyl)(1,2,5,6-η-octafluorocyclooctatetraene)rhodium(I) (5) and (μ-(1,5,6-η:2-4-η)-Octafluorocyclooctatrienediyl)bis[(η^5-indenyl)rhodium](*Rh–Rh*) (12). To a stirred solution of OFCOT (0.90 g, 3.6 mmol) in hexane (25 mL) was added Rh(η^5-C_9H_7)(C_2H_4)$_2$ (0.90 g, 3.6 mmol). The reaction mixture was heated to reflux for 4 days during which time a red solid formed on the side of the flask. The yellow mother liquor was decanted off of the red solid, and the solvent was removed under reduced pressure. Column chromatography of the residue on silica gel (2 × 40 cm) (hexane, 180 mL) followed by removal of the solvent yielded **5** (0.05 g, 3%). Recrystallization of a portion of this material from hexane at −20 °C led to crystals that were suitable for X-ray diffraction studies (see below). **5**: ^{19}F NMR (acetone-d_6, 25 °C) δ 115.9 (m, $F_{2,3}$), 165.1 (m, $F_{1,4}$); ^1H NMR (acetone-d_6, 25 °C) δ 6.12 (d, $H_{1,3}$, $J_{1,2}$ = 3.0 Hz), 6.57 (t, H_2, $J_{1,2}$ = 3.0 Hz, J_{Rh-H_2} = 3.0 Hz), 7.60 (m, H_{4-7}); ^{19}F NMR (toluene-d_8, −90 °C) δ 118.2 (br, F_3), 120.4 (br, F_2), 164.2 (br, F_4), 174.5 (br, F_1); ^1H NMR (toluene-d_8, −125 °C) δ 4.89 (br, H_{1-3}), 6.93–7.3 (m, H_{4-7}); $^{13}C\{^1H\}$ NMR [taken at the University of Waterloo on a Bruker AM250 spectrometer] (CD_2Cl_2) 88.32 (s, $C_{1,3}$), 96.64 (d, C_2, J_{Rh-C} = 4.2 Hz), 106.30 (d, $C_{8,9,12,13}$, $^1J_{F-C}$ = 289.9 Hz), 115.40 (s, $C_{3a,7a}$), 122.34 (s, $C_{5,6}$), 129.12 (s, $C_{4,7}$), 138.2 (d, $C_{10,11,14,15}$, $^1J_{F-C}$ = 290.9 Hz). Elemental composition was confirmed by an X-ray diffraction study.

The red solid was purified by an 18-h Soxhlet extraction with hexane (80 mL). The hexane extract was evaporated under reduced pressure, and the residue was crystallized from THF/

(27) Van Geet, A. L. *Anal. Chem.* **1968**, *40*, 2227–2229.
(28) Piccini-Leopardi, C.; Fabre, O.; Reisse, J. *Org. Magn. Reson.* **1976**, *8*, 233–236.

hexane at −20 °C to yield red crystals (0.88 g, 71%). Recrystallization of a portion of this material from methylene chloride/hexane at −20 °C led to crystals that were suitable for X-ray diffraction studies (see below). **12**: mp 196–198 °C dec; ^{19}F NMR (CH_2Cl_2, 25 °C) δ 119.72 (br, 2 F), 151.06 (br, 4 F), 179.43 (br, 2 F); ^{1}H NMR ($CDCl_3$, 25 °C) δ 5.85 (br, 1 H), 5.91 (m, 1 H), 6.51 (m, 2 H), 6.56 (m, 1 H), 7.38–7.55 (m, 7 H), 7.87–7.90 (m, 2 H); IR (KBr) $\nu_{C=C}$ 1718 cm^{-1}; MS, *m/e* 684 (M^+). Anal. Calcd for $C_{26}H_{14}F_8Rh_2$: C, 45.64; H, 2.06. Found: C, 45.35; H, 2.39.

Repeating the reaction in THF as a solvent led to a deep red homogeneous solution which was worked up in the same manner to yield both **5** and **12** (**5**, 12%; **12**, 74%).

Variable-Temperature NMR Studies of 12. A solution of **12** (0.020 g, 0.03 mmol) in acetone-d_6 (0.5 mL) was subjected to low-temperature ^{1}H and ^{19}F NMR spectroscopy studies. At −90 °C, a limiting ^{19}F NMR spectrum was reached that showed eight major resonances of equal intensity and eight smaller resonances, presumably due to a minor structural isomer as discussed in the text. **12** (major isomer): ^{19}F NMR (acetone-d_6, −90 °C) δ 113.9 (m, F_3), 125.7 (m, F_2), 147.2 (m, F_5), 154.7 (m, F_6), 155.3 (m, F_7), 172.8 (m, F_8), 177.8 (m, F_1), 188.9 (m, F_4); ^{1}H NMR (acetone-d_6, −90 °C) δ 5.2 (br, 1 H), 5.9 (br, 1 H), 6.0 (br, 1 H), 6.5 (br, 1 H), 6.79 (br, 1 H), 7.0–7.4 (m, 8 H). **12** (minor isomer): ^{19}F NMR (acetone-d_6, −90 °C) δ 115.8 (m, 1 F), 127.4 (m, 1 F), 133.8 (m, 1 F), 143.0 (m, 1 F), 154.3 (m, 2 F), 172.3 (m, 1 F), 185.1 (m, 1 F). A solution of **12** (0.020 g, 0.03 mmol) in toluene-d_8 (0.5 mL) was subjected to high-temperature ^{1}H and ^{19}F NMR spectroscopy studies. At 110 °C, the high-temperature limit spectrum was reached which showed four resonances in the ^{19}F NMR spectrum and two sets of indenyl resonances in the ^{1}H NMR spectrum. **12**: ^{19}F NMR (toluene-d_8, 110 °C) δ 119.2 (br s, $F_{3,2}$), 151.6 (br s, $F_{6,7}$), 168.4 (br s, $F_{5,8}$), 178.3 (br s, $F_{1,4}$); ^{1}H NMR (toluene 110 °C) δ 5.31 (br, 1 H), 5.33 (d, 2 H), 5.58 (d, 2 H), 5.80 (t, 1 H), 7.4–7.9 (m, 8 H). Line-shape analyses were carried out on this formally eight-spin system by treating each set of exchanging F sites as an individual pair. Since the chemical shift separations are very large compared to the magnitude of the F–F coupling constants, the latter were approximated as zero in the analysis.

Variable-Temperature NMR Studies of (η^5-Indenyl)-(1,2,5,6-η-cyclooctatetraene)rhodium(I) (10). Complex **10** was prepared by the method of Green.[8] The ^{1}H NMR spectrum of the isolated material at room temperature matched the literature report. A clean, dry, 5-mm NMR tube fitted with a septum was charged with **10** (0.05 g, 0.15 mmol), and the tube was immersed in a −90 °C dry ice/acetone bath. Freon 22 ($CHClF_2$) (bp −44 °C) was passed through a 4-Å molecular sieve trap and condensed into the NMR tube. After approximately 0.3 mL of solvent had been condensed, acetone-d_6 (0.02 mL) was added to the yellow solution as a lock solvent. The NMR tube was placed into the precooled NMR probe (−75 °C), and ^{1}H NMR spectra were recorded from −75 to −140 °C. **10**: ^{1}H NMR (C_6D_6, 25 °C) δ 4.12 (s, $H_{8,9,12,13}$), 4.73 (d, $H_{1,3}$, J_{Rh-H} = 2.6 Hz), 5.60 (s, $H_{10,11,14,15}$), 5.93 (d, H_2, J_{Rh-H} = 0.5 Hz), 7.07 (m, H_{4-7}); ^{1}H NMR (−140 °C, $CHClF_2$/acetone-d_6) δ 3.90 (br, $H_{8,9}$), 4.40 (br, $H_{12,13}$), 5.15 (br, $H_{1,3}$), 5.37 (br, $H_{10,15}$), 5.71 (br, $H_{11,14}$), 6.10 (br, H_2), 6.7–7.7 (m, H_{4-7}).

Formation of (μ-(1,2,5,6-η:3,4,7,8-η)-Cyclooctatetraene)-bis[(η^5-indenyl)rhodium] (11). To a stirred solution of Rh-(η^5-C_9H_7)(C_2H_4)$_2$ (0.20 g, 0.73 mmol) in THF (5 mL) was added COT (purified by filtration through alumina, 0.040 mL, 0.36 mmol). The reaction mixture was heated to reflux for 4 days. The solvent was removed under reduced pressure, and the residue was dissolved in THF. The THF solution was cooled to −20 °C, and a green-yellow solid was formed. The solid was extracted with Et_2O (7 × 20 mL), and the extracts were cooled to −20 °C. Bright yellow crystals were formed which were rinsed with hexane to give **11** (0.05 g, 25%). **11**: mp 238–240 °C dec; ^{1}H NMR (acetone-d_6) δ 4.38 (d, H_{8-15}, J_{Rh-H} = 1.5 Hz), 4.92 (d, $H_{1,2,16,18}$, J_{Rh-H} = 3.0 Hz), 6.06 (d, $H_{2,17}$, J_{Rh-H} = 1.7 Hz), 7.03–7.15 (m, $H_{4-7,19-22}$); IR (KBr) ν_{C-H} 2990, $\nu_{C=C}$ 1340 cm^{-1}. Anal. Calcd for $C_{26}H_{22}Rh_2$: C, 57.80; H, 4.10. Found: C, 57.80; H, 4.18%.

Bis[(η^5-indenyl)(μ-(1,2,5,6-η:7,8-η)-octafluorocyclo-octatetraene)carbonyldirhodium] (18). Carbon monoxide was bubbled through a stirred solution of **12** (0.07 g, 0.1 mmol) in THF (10 mL) at a rate of ~1 bubble/s. The red solution turned yellow within 10 min. The bubbling was continued for an additional 20 min, and the solvent was then removed under reduced pressure. A ^{19}F NMR spectrum of the yellow oily residue revealed two sets of four resonances: one set (δ 111.3, 119.9, 138.2, 169.2) presumably due to a major isomer and the second set (δ 117.2, 118.8, 135.5, 176.3) due to a minor isomer as discussed in the text. The deep yellow oil was crystallized from methylene chloride/hexane at −20 °C. Yellow crystals were isolated (0.05 g, 70%), and the ^{19}F NMR spectrum indicated the material was the major isomer. Single crystals were subjected to X-ray diffraction studies (see below). **18**: mp 174–175 °C; ^{19}F NMR (toluene-d_8, 0 °C) δ 111.3 (br, F_4), 119.9 (d, F_1), 138.2 (t, F_3), 169.2 (t, F_2), $J_{1,2}$ = 28, $J_{2,3}$ = 28, $J_{3,4}$ = 28 Hz; ^{1}H NMR (toluene-d_8) δ 5.5 (br, 1 H), 6.10 (br, 2 H), 6.3 (br, 2 H), 6.7 (br, 1 H), 7.3–7.9 (m, 8 H); IR ($CDCl_3$) $\nu_{C\equiv O}$ 2055, 2025, $\nu_{C=C}$ 1726 cm^{-1}. Elemental composition was confirmed by an X-ray diffraction study. Heating a solution of **18** in benzene-d_6 resulted in re-formation of **12** as evidenced by ^{19}F NMR spectroscopy.

Bis[(η-indenyl)(μ-(1,2,5,6-η:7,8-η)-octafluorocyclo-octatetraene)(ethylene)dirhodium] (20). Ethylene was bubbled through a stirred solution of **12** (0.025 g, 0.035 mmol) in THF (10 mL) at a rate of ~1 bubble/s. The red solution turned yellow within 30 min. A ^{19}F NMR spectrum of the solution indicated almost complete conversion to **20**: ^{19}F NMR (THF) δ 120.3 (d, F_4), 133.2 (t, F_1), 135.0 (d, F_3), 171.2 (t, F_2). This material readily reverted to **12** on attempts to recrystallize it.

Chromatography of 12. Formation of Bis[(η-indenyl)-(μ-(1,2,5,6-η:2-4-η)-5-hydroheptafluorocyclooctatetraene)di-rhodium](*Rh–Rh*) (21). Silica Gel. On a water cooled silica gel column (2.5 × 55 cm) packed in hexane was placed **12** (0.20 g, 0.03 mmol) in CH_2Cl_2 (5 mL). Elution with THF/Et_2O (70:30), followed by removal of the solvent under reduced pressure, gave a red oil (0.17 g, 85%) which was crystallized from THF/CH_2Cl_2 at −20 °C to give single crystals which were subjected to X-ray diffraction studies. Spectroscopy was also performed on the crystallized material. **21**: mp 178–180 °C; ^{19}F NMR (acetone-d_6, 25 °C) δ 116.03 (m, F_2), 125.3 (m, F_1), 140.3 (m, F_5), 147.2 (m, F_4), 154.1 (m, F_6), 179.8 (m, F_8), 185.0 (m, F_3); ^{1}H NMR (acetone-d_6) δ 4.6 (br, 1 H), 5.43 (d, 1 H, J_{Rh-H} = 1.0 Hz), 5.82 (m, 1 H), 5.86 (s, 1 H), 6.29 (m, 1 H), 6.46 (m, 1 H), 6.7 (m, 1 H), 7.0–7.9 (m, 8 H); IR (THF): $\nu_{C=C}$ 1743 cm^{-1}; MS, *m/e* 666 (M^+). Anal. Calcd for $C_{26}H_{15}F_7Rh_2$: C, 46.88; H, 2.27. Found: C, 47.28; H, 2.26.

Subsequent elution with acetone, followed by removal of the solvent under reduced pressure, gave a red oil (<0.002 g). **22**: ^{19}F NMR (toluene-d_8), δ 101.5 (1 F), 116.7 (1 F), 118.0 (1 F), 121.5 (1 F), 147.5 (1 F), 166.5 (2 F).

Complex **22** could also be produced by heating a solution of **21** in toluene-d_8 to 115 °C in an NMR tube and monitoring the conversion by ^{19}F NMR spectroscopy. Additional unidentified ^{19}F NMR resonances were also observed.

Rapid Elution. On a water-cooled silica gel column (2.5 × 55 cm) packed in hexane was placed **12** (0.1 g, 0.3 mmol) in CH_2Cl_2 (5 mL). Immediate elution with acetone (contact time of approximately 10 min) gave **12** as monitored by ^{19}F NMR spectroscopy.

Alumina. On an water-cooled alumina column (2 × 14 cm) packed with hexane was placed **12** (0.010 g, 0.015 mmol). Elution with acetone produced a red band that was collected. A ^{19}F NMR spectrum of the acetone fraction showed **21** and **22**.

Attempted Reaction of 12 with Acids. Tetrafluoroboric Acid–Diethyl Ether. In a dry 5-mm NMR tube was placed **12** (0.021 g, 0.03 mmol) in THF (0.2 mL). HBF_4·Et_2O (4.4 μL, 0.03 mmol) was added via a gas-tight syringe. The mixture was monitored by ^{19}F NMR spectroscopy and showed only resonances due to **12** after 24 h.

Trifluoroacetic Acid. In a dry 5-mm NMR tube was placed **12** (0.005 g, 0.007 mmol) in $CDCl_3$ (0.2 mL). CF_3COOH (6.0 μL, 0.007 mmol) was added via a gas-tight syringe. The mixture was monitored by ^{19}F NMR spectroscopy and showed only resonances due to **12** and the trifluoroacetic acid after 24 h.

X-ray Crystallographic Determinations. (η^5-Indenyl)-(1,2,5,6-η-octafluorocyclooctatetraene)rhodium(I) (5). $C_{17}H_7F_8Rh$: mol wt 466.138; triclinic, $P\bar{1}$, a = 8.445 (1) Å, b = 8.850 (1) Å, c = 10.142 (1) Å, α = 85.22 (1)°, β = 81.63 (1)°, γ = 89.35 (1)°, V = 747.3 (2) Å^3, Z = 2, ρ_{calcd} = 2.071 g cm^{-3}; $F(000)$ = 452; T = 294 ± 1 K; λ = 0.710 69 Å; μ(Mo Kα) = 12.13 cm^{-1}. A crystal of dimensions 0.22 × 0.22 × 0.24 mm was mounted on

a Syntex $P2_1$ diffractometer. Accurate cell parameters were determined from 15 general reflections well dispersed in reciprocal space. Data were collected via the θ–2θ scan method ($2\theta \leq 50°$) using variable scan rates (3.45–29.30° min^{-1}) and a scan width of 0.8° below $K\alpha_1$ to 0.8° above $K\alpha_2$. Background counts were made at the beginning and end of each scan for a time equal to half the scan time. The intensities of two standard reflections 400; 005) were monitored every 100 measurements. These exhibited only minor fluctuations. The data were corrected for Lorentz and polarization effects, but since $\mu = 12.13$ only and since the crystal was of regular dimensions, no absorption correction was deemed necessary. From a total of 2663 measured intensities, 2482 with $I \geq 3\sigma(I)$ were considered observed and used in the structure solution and refinement. The structure was solved by Patterson and Fourier techniques and refined by full-matrix least-squares methods. With all non-hydrogens isotropic an R of 0.066 was obtained ($R = \sum||F_o| - |F_c||/\sum|F_o|$. Conversion to anisotropic thermal parameters and subsequent inclusion of hydrogen atoms resulted in convergence at $R = 0.0207$ and $R_w = 0.0241$ ($R_w = [\sum w(|F_o| - |F_c|)^2/\sum w|F_o|^2]^{1/2}$). In the final cycles an empirical weighting scheme of the form $w^{-1} = 2.12 - 0.052|F_o| + 0.0015|F_o|^2$ was applied. A final difference Fourier was featureless with maximum residuals of 0.35 e $Å^{-3}$ in the vicinity of the rhodium atom. A final GOF (defined as $[\sum w(|F_o| - |F_c|)^2/(N_o - N_v)]^{1/2}$) of 0.40 was obtained for 264 variables. Scattering factor tables including corrections for the anomalous scattering of rhodium were taken from ref 29.

Bis[(η-indenyl)(μ-(1,5,6-η:2-4-η)-octafluorocyclooctatrienediyl)dirhodium](*Rh–Rh*) (12) and Bis[(η-indenyl)(μ-(1,5,6-η:2-4-η)-5-hydroheptafluorocyclooctatetraene)dirhodium](*Rh–Rh*) (21). Data relating to the crystals, data collection, and refinement are presented in Table VI. Except as noted the two structures were determined similarly. Specimens were mounted on glass fibers and the crystal system and space group obtained from preliminary photographic and intensity measurements. The unit cell parameters were obtained from the best fit of the angular settings of 25 reflections ($22° \leq 2\theta \leq 32°$). Empirical methods (216 data) were used to correct for absorption. The structures were solved by direct methods and completed by subsequent difference Fourier syntheses. For complex **12** the indenyl group at Rh(2) is disordered, causing a displacement of Rh(2) by ~0.8 Å. Refinement of the occupancies of Rh(2) and Rh(2′), the displaced atom, revealed 89% and 11% occupancies, respectively. No attempt was made to refine the displaced indenyl carbon positions, but about half of the atoms were present in the final difference map. All non-hydrogen atoms, except Rh(2′) in complex **12**, were anisotropically refined. Hydrogen atom contributions were idealized [d(C–H) = 0.96 Å], except for H(8) in complex **21** which was located and isotropically refined. SHELXTL (5.1) software (Nicolet Corp., Madison, WI) was used for all computations and served as the source for scattering factors.

Bis[(η^5-indenyl)(μ-(1,2,5,6-η:7,8-η)-octafluorocyclooctatetraene)carbonyldirhodium] (18). Crystal data collection and refinement parameters are provided in Table IX. Preliminary photographic characterization showed no symmetry greater than triclinic, and this was confirmed by TRACER. The centrosymmetric space group $P\bar{1}$ was initially assumed and later proved correct by the computational stability of the refinement process. No correction for absorption was required (average $T_{max}/T_{min} = 1.07$). The structure was solved by an automated Patterson interpretation after the failure of direct methods to locate the two Rh atoms. Further development of the structure proceeded normally via a series of difference Fourier syntheses. All non-hydrogen atoms were refined with anisotropic thermal parameters. Hydrogen atoms were treated as idealized, isotropic updated contributions. All computations used the SHELXTL (5.1) program library (Nicolet Corp., Madison, WI).

Acknowledgment. R.P.H. is grateful to the Air Force Office of Scientific Research (Grant AFOSR-86-0075), the donors of the Petroleum Research Fund, administered by the American Chemical Society, and the National Science Foundation for generous support of this work. The loan of rhodium trichloride by Johnson Matthey Inc. is also gratefully acknowledged. T.B.M. thanks the Natural Sciences and Engineering Research Council of Canada and Imperial Oil Ltd. for partial support of the work done at Waterloo and E.I. duPont de Nemours and Co. Inc. for a generous donation of materials and supplies.

Registry No. 1, 57070-35-6; 5, 96688-73-2; 9, 63428-46-6; 10, 74436-27-4; 11, 114325-48-3; 12, 114350-51-5; 18, 114350-52-6; 20, 114325-49-4; 21, 114325-50-7.

Supplementary Material Available: Tables of bond distances and angles, and anisotropic thermal parameters for **5**, **12**, **18**, and **21** and hydrogen-atom coordinates for **12**, **18**, and **21** (20 pages); listings of observed and calculated structure factors for **5**, **12**, **18**, and **21** (80 pages). Ordering information is given on any current masthead page.

(29) *International Tables of X-ray Crystallography*; Kynoch: Birmingham, England, 1974; Vol. 4.